

### 5A.1. *N*3 aryl/heteroaryl substituted 2-(2-chlorostyryl)-6,7-dimethoxy-quinazolin-4(3*H*)-ones (5a-5l) (Series-I)

#### 5A.1.1. Chemistry

The compounds were synthesized by three-step method. The primary two steps involve amidation and intramolecular cyclization to form the 2-(2-chlorostyryl)-6,7-dimethoxy-4*H*-benzo[*d*][1,3]oxazin-4-one ring. Thereafter, the compounds **5a-5l** were obtained by the fusion of various substituted aryl/heteroarylamines with 2-(2-chlorostyryl)-6,7-dimethoxy-4*H*-benzo[*d*][1,3]oxazin-4-one. The structures of compounds were characterised by FT-IR, <sup>1</sup>H NMR, <sup>13</sup>C NMR and elemental analysis. The mass of representative compounds were determined by mass spectroscopy. Elemental analysis results were within  $\pm 0.4\%$  of the theoretical values and the spectral data are in agreement with the structures of the synthesized compounds. The spectra of the intermediate (**3**) displayed the characteristic  $\text{C}=\text{O}$  stretch of amide and  $\text{COOH}$  group at 1685 and 1732  $\text{cm}^{-1}$  respectively. A broad peak was observed at 3437  $\text{cm}^{-1}$  due to  $\text{NH}$  stretch and the  $\text{C}=\text{O}$  stretch of cyclic ester of the intermediate (**4**) was observed at 1735  $\text{cm}^{-1}$ . All the derivatives showed absorptions at 1595–1608  $\text{cm}^{-1}$  due to the presence of  $\text{C}=\text{N}$  bond and the  $\text{C}=\text{O}$  stretching of the quinazolin-4(3*H*)-one nucleus was observed at 1629–1674  $\text{cm}^{-1}$ .

The non-magnetically equivalent ethylene protons exhibited a common spectral range each appearing as a doublet. The coupling constant between the ethylene protons is in the range of 11.7–16.5 Hz and indicate  $J_{trans}$  coupling. The methoxy protons displayed signals at  $\delta$  3.89–4.00 ppm and all the other protons belonging to the methyl and aromatic ring were observed according to the expected chemical shift. The <sup>13</sup>C NMR peaks corresponding to  $\delta$  159.26–163.26 ppm suggested the presence  $\text{C}=\text{O}$  group of quinazolin-4(3*H*)-ones and the  $\text{OCH}_3$  peak appear at around  $\delta$  56 ppm. The aromatic carbons appear at around  $\delta$  121–134 ppm and all the other <sup>13</sup>C NMR peak were seen according to the expected chemical shift. The partition coefficient and solubility of the synthesized compounds were also determined.

#### 5A.1.2. Pharmacological activity

The anticonvulsant activity of the synthesized compounds (**5a-5l**) was assessed using MES, *sc*PTZ and AMPA induced seizure models. These acute seizure models are widely utilised for preclinical assessment of potential anticonvulsant drugs. The MES

test involves transauricular or transcorneal electrical induction whereas *sc*PTZ and *icv* AMPA involves chemical induction of generalized seizure. The ED<sub>50</sub> values are listed in Table 5A.1. and the results were compared with those of phenytoin, GYKI 52466 and talampanel. The standards GYKI 52466 and talampanel were included in the study to correlate the anticonvulsant activity of the compounds with standard AMPA receptor antagonist. The effect on motor coordination was examined by the rotarod test. Few of the compounds demonstrated their ability to prevent seizure spread in the models used for the present *in vivo* screening.

The *N*3 phenyl (**5a**) and 3-methoxyphenyl (**5e**) derivative of quinazolin-4(3*H*)-one were found to be the least active compounds against all seizure models compared to the other quinazolin-4(3*H*)-ones derivatives within the series-I. In MES test, it was found that a methylene linkage (**5f**) in between the phenyl ring and quinazolin-4(3*H*)-one nucleus tends to increase the potency moderately. Potent activity was shown by mono substitution of methyl group (**5c**) at the *meta* position of *N*3 aryl moiety while disubstitution of the methyl group (**5b**) results in a considerable decrease in activity.

Taking into account the compounds with *N*3 heteroaryl substitution, the pyridin-4-yl derivative (**5k**) showed good activity (ED<sub>50</sub> 66.4 μmol/kg) against MES-induced seizure. Among all the compounds, **5g** and **5i** exhibited promising activity. In particular, **5g** with *N*3 *para* nitrophenyl substitution with an ED<sub>50</sub> of 41.3 μmol/kg demonstrated comparable potency as that of GYKI 52466.

Unlike **5g**, a difference in activity was observed with the *N*3 *ortho* nitrophenyl (**5h**) derivative (ED<sub>50</sub> 98.2 μmol/kg). Investigational anticonvulsant drugs are initially screened for efficacy in both MES and *sc*PTZ tests. Therefore, based on the level of activity obtained in MES test, few compounds (**5c**, **5g**, **5i** and **5k**) were selected for assessment against *sc*PTZ induced seizure. In contrary to anticonvulsant activity against MES induced seizure, the *N*3 *para* bromophenyl derivative (**5i**) elicited highest potency against *sc*PTZ induced seizure. The other compounds displayed a parallel activity pattern as obtained from MES test and the activity is dose-dependent and an increase in dose was required to protect against *sc*PTZ induced seizure.

To establish the mechanism, all the compounds were subjected to AMPA induced seizure test. It explain whether the designed compounds exhibit anticonvulsant action by interacting with the AMPA receptors at the sites innervated with the receptors under consideration. The order of potency against AMPA induced seizure was found to follow the similar pattern as those observed against MES induced seizure.

However, the potencies of **5k** in *sc*PTZ and AMPA induced seizure test was found to be similar. In AMPA induced seizure, the ED<sub>50</sub> value of **5g** was 50.3 μmol/kg and under the present experimental condition, the potency of **5g** was comparable with talampanel. These observations indicate that substitution of electron withdrawing group at the *para* position of *N*3 aryl ring demonstrated better anticonvulsant activity with significantly low impairment of rotarod performance in mice compared to the *N*3 aryl derivatives substituted with electron donor groups (**5d** and **5e**). From the findings, it can also be assumed that the substituted aryl/heteroaryl ring at the *N*3 position of a 6,7-dimethoxyquinazolin-4(3*H*)-one nucleus have crucial modulatory effects on anticonvulsant activity. Among all compounds in the series-I, **5g** demonstrated promising anticonvulsant actions in various seizure models with desirable protective index.

**Table 5A.1.** Anticonvulsant activity of compounds **5a–5l** against MES, *sc*PTZ and AMPA induced seizure in Swiss albino mice. TD<sub>50</sub> assessed by rotarod test.

Compd	<sup>a</sup> ED <sub>50</sub> (μmol/kg)			<sup>a</sup> TD <sub>50</sub> (μmol/kg) Rotarod	PI
	MES	<i>sc</i> PTZ	AMPA		
5a	135.1 (97.4–189.7)	ND	150.9 (76.8–269.6)	229.6 (186.3–276.2)	1.7
5b	109.4 (66.8–148.8)	ND	119.8 (87.4–160.1)	306.3 (225.5–321.3)	2.8
5c	59.7 (20.0–99.1)	90.2 (54.2–132.7)	69.8 (42.5–97.2)	160.0 (109.0–265.7)	2.6
5d	103.0 (60.8–161.1)	ND	120.8 (53.3–226.1)	136.2 (94.3–202.9)	1.3
5e	134.8 (98.3–186.6)	ND	146.3 (107.5–205.9)	213.3(151.2–382.7)	1.5
5f	88.0 (65.4–106.9)	ND	95.8 (70.5–120.2)	155.9 (110.2–238.9)	1.7
5g	41.3 (26.1–63.4)	82.5 (60.9–99.6)	50.3 (25.9–73.1)	212.8 (148.6–396.7)	5.1
5h	98.2 (59.2–148.1)	ND	105 (77.6–136.3)	201.9 (144.4–344.7)	2.0
5i	52.3 (26.2–76.9)	72.7 (51.9–90.9)	66.3 (44.1–87.4)	228.7 (150.6–312.9)	4.3
5j	94.6 (44.4–132.0)	ND	114.3 (86.1–145.3)	160.1 (87.6–265.7)	1.6
5k	66.4 (34.0–99.2)	75.3 (40.3–112.9)	72.7 (51.9–90.9)	135.1 (98.5–186.6)	2.0
5l	93.9 (54.9–142.5)	ND	118.6 (88.3–154.1)	111.3 (77.7–144.7)	1.1
GYKI 52466	35.9 (27.1–63.3)	68.7 (41.7–95.8)	41.5 (14.8–66.1)	76.0 (34.4–122.6)	2.1
PNT	15.7 (7.2–28.3)	23.7 (12.2–42.4)	–	85.2 (50.2–126.0)	5.4
TLP <sup>b</sup>	28.8	56.3	40.5	–	–

<sup>a</sup>ED<sub>50</sub> and TD<sub>50</sub> values were calculated by probit method (95% confidence limits are given in parentheses).

PI–protective index indicates TD<sub>50</sub> of rotarod/ED<sub>50</sub> of MES.

ND: activity not determined.

PNT:Phenytoin; TLP:Talampanel

<sup>b</sup>Data from De Sarro *et al.*, 2003.

### 5A.1.3. Hepatotoxicity study

The hepatotoxicity assessment was carried out with the view that liver plays an important role in the metabolism of the majority of neuro-active drugs. It is also true that any associated liver disease can adversely affect the biotransformation of some of

these drugs. Compounds showed no significant change in the activities of enzymes (AST and ALT) as compared to the control animals (Table 5A.2). The control and the test groups (**5g**, **5i** and **GYKI 52466**) were also examined histopathologically and showed no focal or diffuse necrosis of hepatocytes. Further, infiltrations of chronic inflammatory cells were also not observed (Figure 5A.1) compared to the control and the standard group. Thus, it can be anticipated that the selected compounds are devoid of hepatotoxicity which is one of the major adverse effects associated with the use of some anticonvulsant drugs (Björnsson, 2008; Ahmed and Siddiqi, 2006).

**Table 5A.2.** Effects of compounds (5g and 5i) on serum AST and ALT of rats

Treatment	AST (U/mL)	ALT (U/mL)
Control	94.53±2.53	37.97 ±2.13
5g	92.17±2.48	38.26 ±2.51
5i	95.76±2.53	42.10 ±2.06
GYKI 52466	94.69±2.98	37.47±2.04

Values are Mean±SD. [One-way analysis of variance (ANOVA) followed by post hoc Tukey's test]. Values were not significant ( $p>0.05$ ) and indicate the non-hepatotoxic nature of the synthesized compounds.

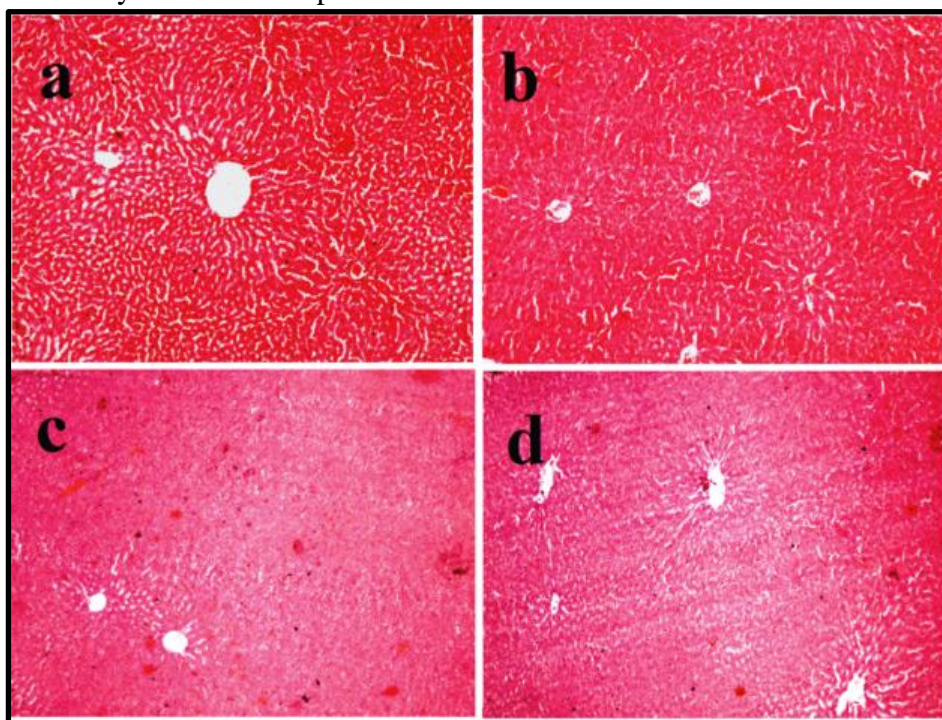


**Figure 5A.1.** Photomicrograph of liver of control (a), compound 5g (b), 5i (c) and GYKI 52466 (d) treated groups at 40X.

### 5B.1. N3 aryl/heteroaryl substituted 2-((benzyloxy and phenylthio) methyl) 6,7-dimethoxyquinazolin-4(3H)-ones (Series-II)

#### 5B.1.1. Chemistry

The compounds were synthesized by three-step method and the initial two steps include amidation followed by intramolecular cyclization to form the benzoxazin-4-one ring. The final step that leads to the formation of the compounds **8a–8l** involves the fusion of various substituted aryl/heteroarylamines with 2-((benzyloxy)methyl)-6,7-dimethoxy-4H-benzo[d][1,3]oxazin-4-one (**8a–8j**) and 2-((phenylthio)methyl)-6,7-dimethoxy-4H-benzo[d][1,3]oxazin-4-one (**8k–8l**). Elemental analysis (C, H and N) and the spectroscopic data were in agreement with the structures of the synthesized compounds. The elemental analysis results were within  $\pm 0.4\%$  of the theoretical values. The characteristic  $\text{C}=\text{O}$  stretchings of amide of intermediates **4** and **5** were observed around 1681 and 1683  $\text{cm}^{-1}$  while the  $\text{C}=\text{O}$  stretching of  $\text{COOH}$  group appeared at 1725 and 1718  $\text{cm}^{-1}$  respectively. Additionally, broad peaks at 3081 and 3087  $\text{cm}^{-1}$  for the intermediates **4** and **5** suggest  $\text{OH}$  stretchings of  $\text{COOH}$  group. The presence of cyclic ester functionality of intermediate **6** and **7** was indicated by  $\text{C}=\text{O}$  stretching at 1737  $\text{cm}^{-1}$  and 1735  $\text{cm}^{-1}$  respectively and supported the formation of benzo[d][1,3]oxazin-4-one ring.

The FT-IR spectra of the synthesized compounds (**8a–8l**) showed the characteristic strong bands for  $\text{C}=\text{O}$  stretching of quinazolin-4(3H)-one at a range of 1674–1683  $\text{cm}^{-1}$  along with a moderate band for  $\text{C}=\text{N}$  stretching at a range of 1604–1612  $\text{cm}^{-1}$ . The spectral range at 1122–1131  $\text{cm}^{-1}$  could be assigned to the  $\text{C}-\text{O}-\text{C}$  stretching for compounds **8a–8j** and a weak  $\text{C}-\text{S}-\text{C}$  stretching was observed at 680 and 678  $\text{cm}^{-1}$  for compounds **8k** and **8l** respectively. The intermediates **4** and **5** displayed a broad singlet at  $\delta$  11.34 and 11.23 ppm respectively for  $\text{OH}$  proton of  $\text{COOH}$  with a set of multiplets were observed at  $\delta$  7.59–7.31 for the aromatic protons.

The two  $\text{CH}_2$  protons of compounds **8a–8j** attached to quinazolin-4(3H)-one ring appear at two common sets of spectral range  $\delta$  4.69–4.75 ppm and  $\delta$  4.12–4.37 as singlet. The  $\text{SCH}_2$  peak of compounds **8k** and **8l** appear at upfield at  $\delta$  3.73 and  $\delta$  3.71 ppm respectively probably due to less electronegative nature of the thio group than the corresponding oxy linkage of C2 benzyloxymethyl derivatives of 6,7-dimethoxyquinazolin-4(3H)-ones. The methoxy protons displayed signals at  $\delta$  3.84–3.98 ppm and the signals of two protons of quinazolin-4(3H)-one ring appear in the

range of  $\delta$  7.13–7.31 for compounds **8a–8j** while the signals appear in the region of  $\delta$  6.95–7.17 ppm for compounds **8k–8l**. All the other protons belonging to the methyl groups and aromatic rings were observed according to the expected chemical shift.

### 5B.1.2. Pharmacological activity

The synthesized compounds (**8a–8l**) were evaluated for their anticonvulsant activity against MES, *sc*PTZ and AMPA-induced seizure model. The effect on motor coordination was examined by using the rotarod test. The compounds were administered *ip* at various doses in the range of 20–500  $\mu\text{mol/kg}$  body weight and their anticonvulsant properties are expressed in terms of  $\text{ED}_{50}$  (Table 5B.1). The standard GYKI 52466 and talampanel were included in the study to correlate the anticonvulsant activity of the compounds with known AMPA receptor antagonists. Some of the compounds demonstrated their ability to prevent the seizure spread in the present *in vivo* screening. The *N*3 benzyl derivative (**8e**) was found to be the least active considering the level of activity against all the seizure models followed by the compounds **8j**, **8b**, **8l** and **8i**. The *N*3 *m*-tolyl derivative (**8a**) displayed a two-fold increase in the potency than the corresponding 2,4 dimethylphenyl derivative (**8b**) against MES induced seizures.

Considering the compounds with *N*3 heteroaryl substitution, the pyridin-4-yl derivative (**8h**) showed good activity ( $\text{ED}_{50}$  70.3  $\mu\text{mol/kg}$ ) against MES-induced seizures with the highest protective index (PI) of 5.2. However, the compounds **8f** and **8k** exhibited promising activity against MES-induced seizures among all the derivatives. This implied that the *para* nitrophenyl substitution at *N*3 position elicits better anticonvulsant activity and is independent of the nature of C2 substituent. This is further confirmed by the fact that the compounds **8c** ( $\text{ED}_{50}$ : 91.2  $\mu\text{mol/kg}$ ) and **8l** ( $\text{ED}_{50}$ : 127.9  $\mu\text{mol/kg}$ ) having a similar *N*3 substitution elicit noticeable difference in the degree of potency. The *N*3 4-bromo phenyl derivative (**8g**) was unable to exhibit desirable activity and brought about a decrease in the level potency.

Based on the level of activity obtained in MES test, few compounds (**8a**, **8f**, **8h** and **8k**) were selected for activity assessment against *sc*PTZ-induced seizure. All of them showed a similar pattern of potency as obtained from MES test and the activity is dose-dependent as an increase in the dose was required to protect against *sc*PTZ-induced seizure similar to series-I. In AMPA-induced seizure model, compound **8f** and **8h** showed more potent with an  $\text{ED}_{50}$  value of 53.0  $\mu\text{mol/kg}$  and 45.6  $\mu\text{mol/kg}$

respectively. Under the present pharmacological screening, the potencies of **8h** and **8f** were comparable to that of the standard AMPA antagonists.

The compound **8f** proved to be the highly potent among all the compounds with a PI of 4.7 and demonstrated activity similar to those of GYKI 52466 against all the seizure models. In summary, the findings indicate that the substitution of the nitro group at the *para* position of the *N3* aryl ring demonstrated better anticonvulsant activity with a significantly low impairment of rotarod performance in mice. From the present investigations, it can also be assumed that the substituted aryl/heteroaryl ring at the *N3* position of a 6,7-dimethoxy-quinazolin-4(3*H*)-one nucleus had a critical modulatory effect on the anticonvulsant activity.

**Table 5B.1** Anticonvulsant activity of compounds **8a–8l** against MES, scPTZ and *icv* AMPA-induced seizure in Swiss albino mice. TD<sub>50</sub> assessed by rotarod test.

Compd	<sup>a</sup> ED <sub>50</sub> (μmol/kg)			<sup>a</sup> TD <sub>50</sub> (μmol/kg) Rotarod	PI
	MES	scPTZ	AMPA		
8a	64.5 (41.2–89.2)	85.9 (62.6–103.4)	95.8 (70.5–120.2)	242.9 (178.7–324.6)	3.7
8b	130.0(93.5–180.8)	ND	139.8 (114.9–171.0)	273.6 (193.7–303.2)	2.1
8c	91.2 (54.2–132.7)	ND	115.6 (79.1–151.5)	282.7 (208.3–314.6)	3.1
8d	116.6 (79.4–134.8)	ND	146.3 (107.5–205.9)	170.5 (114.8–287.9)	1.6
8e	143.9 (116.9–179.3)	ND	183.0 (127.9–311.5)	330.9 (305.2–348.4)	2.3
8f	40.9 (27.1–63.3)	69.8 (42.5–97.2)	53.0 (27.1–77.5)	193.6 (128.0–392.2)	4.7
8g	105.8 (77.6–136.3)	ND	127.4 (98.8–161.2)	190.4 (126.4–356.4)	1.8
8h	70.3 (30.4–112.9)	88.0 (65.4–106.9)	45.6 (23.1–66.4)	197.0 (134.3–372.1)	2.8
8i	123.1 (95.3–154.8)	ND	140.5 (102.6–196.6)	233.8 (143.7–257.5)	1.9
8j	134.8 (98.3–186.6)	ND	155.9 (110.2–238.9)	323.5 (289.4–365.2)	2.4
8k	45.6 (23.1–66.4)	75.1 (53.2–94.5)	59.7 (20.0–99.1)	237.1 (164.1–282.8)	5.2
8l	127.9 (95.4–169.3)	ND	135.1 (97.4–189.7)	422.1 (369.6–469.3)	3.3
GYKI 52466	35.9 (27.1– 63.3)	68.7 (41.7–95.8)	41.5 (14.8–66.1)	76.0 (34.4–122.6)	2.1
PNT	15.7 (7.2–28.3)	23.7 (12.2–42.4)	–	85.2 (50.2–126.0)	5.4
TLP <sup>b</sup>	28.8	56.3	40.5	–	–

<sup>a</sup>ED<sub>50</sub> and TD<sub>50</sub> values were calculated by the probit method (95% confidence limits are given in parentheses). (n=8/group, where n represents the number of mice per group).

PI: protective index indicates TD<sub>50</sub> of rotarod/ED<sub>50</sub> of MES.

ND: activity not determined.

PNT:Phenytoin; TLP:Talampanel

<sup>b</sup>Data from De Sarro *et al.*, 2003.

### 5B.1.3. Hepatotoxicity study

The compounds (**8a–8l**) showed no significant change in the activities of the enzymes as compared to the control group (**Table 5B.2.**). Histopathological examination of control and the representative compounds (**8f** and **8h**) presented no focal or diffuse necrosis of hepatocytes and infiltrations of inflammatory cells were also not detected

(Figure 5B.1.) compared to the control and GYKI 52466 groups. Thus, it could be assumed that the compounds are devoid of any hepatotoxic liability.

**Table 5B.2.** Effects of compounds (8f and 8h) on serum AST and ALT of rats.

Treatment	AST (U/mL)	ALT (U/mL)
Control	94.53±2.53	37.97 ±2.13
8f	93.01±2.55	39.07 ±2.01
8h	96.04±2.50	38.43 ±2.60
GYKI 52466	94.69±2.98	37.47±2.04

Values are Mean±SD. (n=6/group, where n represents the number of mice in a group) [One-way analysis of variance (ANOVA) followed by post hoc Tukey's test]. Values were not significant ( $p>0.05$ ) indicating the non-hepatotoxic nature of the synthesized compounds.

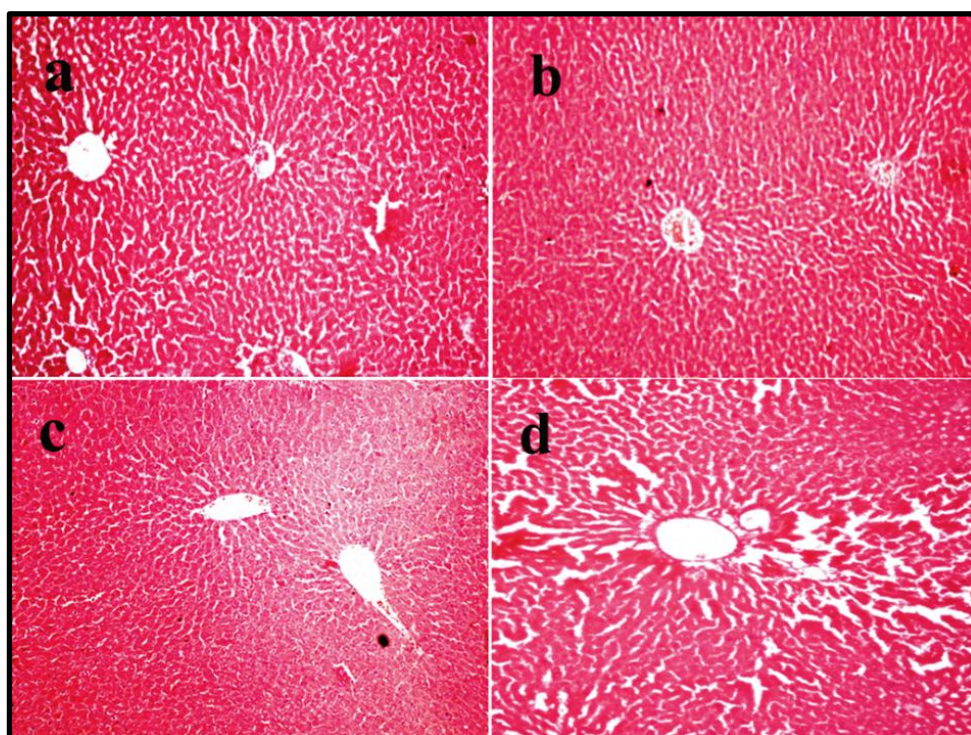


**Figure 5B.1.** Photomicrograph of liver at 40X magnification (a) control, (b) 8f, (c) 8h and (d) GYKI 52466 treated groups revealing intact central vein, hepatocytes and sinusoids.

### 5C.1. Partition coefficient and *in silico* ADME prediction of the synthesized compounds (Series I and II)

The experimentally determined log P values of the synthesized compounds (**5a–5l**, **8a–8l**) were found in the range of 2.14–2.83, and the values (*cf.* Table 4A.2. and Table 4B.2.) were lower than those calculated computationally (Table 5C.1.). In consideration of the lipophilicity of the compounds, the parameter was not able to affect the activity, and no substantial correlation could be drawn between lipophilicity and activity. Nevertheless, log P conforms to the suggested value of  $\log P \leq 5$  and the mean value of the experimental log P was found to be 2.55. This suggests that the synthesized compounds are suitable as CNS drugs (Pajouhesh and Lenz, 2005).

The compounds were also subjected to evaluation by the QikProp<sup>®</sup> (version 3.2) module of the Maestro Schrödinger software for the prediction of their pharmacokinetic properties. All the compounds were neutralized before being subjected to QikProp<sup>®</sup> analysis and the significant pharmacokinetic properties consisting of principal descriptors such as log P (octanol/water), % human oral absorption, Lipinski's rule of five violation, CNS activity, detection of reactive functional groups and brain/blood partition coefficient are reported. The *in silico* study predicted the compounds (**5g**, **5i**, **5k**, **8b**, **8f**, **8h** and **8k**) were active for CNS and also cross the blood–brain barrier. All the compounds obey Lipinski's rules of five. For a drug to be orally active, it should possess no more than one violation (Lipinski, 2004) of the following criteria:

- No more than 5 hydrogen bond donors (the total number of nitrogen–hydrogen and oxygen–hydrogen bonds)
- Not more than 10 hydrogen bond acceptors (including all nitrogen or oxygen atoms)
- A molecular mass less than 500 daltons
- An octanol–water partition coefficient not greater than 5

Further, QikProp<sup>®</sup> predicted the absence of any reactive functional groups and a considerable oral absorption for all the compounds (Table 5C.1; *cf.* Table 4C.2.).

**Table 5C.1.** Pharmacokinetic prediction of selected compounds by QikProp® 3.2

Compd	QPlogPo/w	Rule of five	#rtvFG	CNS	QPlogBB	% Human oral absorption
5g	4.21	0	0	-2	-1.22	100
5i	4.54	1	0	1	0.00	100
5k	4.27	0	0	0	-0.35	100
8b	4.51	0	0	0	-0.22	100
8f	3.24	0	0	-2	-1.04	96.14
8h	3.06	0	0	-1	-0.50	100
8k	3.68	0	0	-1	-0.89	100

### 5C.2. Molecular Modelling study

The templates of the synthesized compounds were based on quinazolin-4(3*H*)-one nucleus as the majority of reported quinazolin-4(3*H*)-ones elicit anticonvulsant activity *via* interaction AMPA receptor site (Menniti *et al.*, 2000; Welch *et al.*, 2001). Therefore, a docking study was carried out on a recently reported crystal structure (PDB: 3SAJ) to find out the putative binding mode within the allosteric amino terminal domain (ATD) of ionotropic glutamate receptor. The LigPrep® module was used to produce the low-energy conformers of the compounds under study. The default values of the parameters of the Glide module were retained. The lowest energy conformation was selected and the ligand hydrogen bonding interactions with the active sites of ATD were obtained. The topmost binding cavity (Figure 4C.1.) predicted by the Sitemap® module of Maestro Schrödinger was in consensus with the previously identified binding site of a reported homology model of leucine/isoleucine/valine binding protein (LIVBP)-like domain of AMPA receptor and this corresponds to the amino terminal domain of the receptor. It is interesting and worth mentioning here that the ratio of the differences of the amino acid residue numbers of the predicted binding cavity were in agreement with the previous reported homology modelled amino terminal domain of AMPA receptor (Table 5C.2.).

The results of the docking study depict an insight into the possible binding mode of the synthesized quinazolin-4(3*H*)-ones. The representative compound **5g**, **8f** and **GYKI 52466** were docked at predicted active site of the ATD domain of AMPA receptor. The binding configuration of **5g** and **8f** showed hydrogen bonding with Arg 108 and Lys 269 (**Figure 5**) with a G score of -6.24 and -6.53 respectively whereas GYKI 52466 was hydrogen bonded to Arg 108 and Ser 188 (G score: -6.31). The hydrogen bond

interaction of the quinazolinone –CO group was found to be with the guanidino group of Arg108. In both the cases, the oxygen atoms from the methoxy group and the 4–oxo group of quinazolin–4(3*H*)–ones served as the hydrogen bond acceptor.

The preferential orientation of the compound **5g**, **8f** and **GYKI 52466** is within the pocket formed due to a cavity–shaping loop, characterised by the amino acid residues viz. Gln 16, Gln 17, Glu 20, His 21, Tyr 71, Ile 91, Arg 108, Ser 188, Phe 217, Met 218, Ile 220, Lys 269, Asp 304, Cys 305, Leu 306 (HB acceptor region). These binding modes corroborate with the suggested ligand–receptor contact points of non–competitive AMPA receptor antagonists reported in the literatures (De Luca *et al.*, 2003; Chimirri *et al.*, 2004). The C2 side chain is skewed towards the hydrophobic region of the receptor site.

**Table 5C.2.** Similarity of amino acid residues within the predicted active site and previously reported homology modelled ATD of AMPA receptor

Sl no.	Amino acid residue number at the active site predicted by Sitemap®	Amino acid residue number by homology modelling (De Luca <i>et al.</i> , 2003)
1.	Gln 16	Gln 34
2.	Gln 17	Gln 35
3.	Glu 20	Glu 38
4.	His 21	His 39
5.	Tyr 71	Tyr 89
6.	Ile 91	Ile 109
7.	Ser 188	Ser 206
8.	Phe 217	Phe 235
9.	Met 218	Met 236
10.	Ile 220	Ile 238
11.	Lys 269	Lys 287
12.	Asp 304	Asp 322
13.	Cys 305	Cys 323
14.	Leu 306	Leu 324

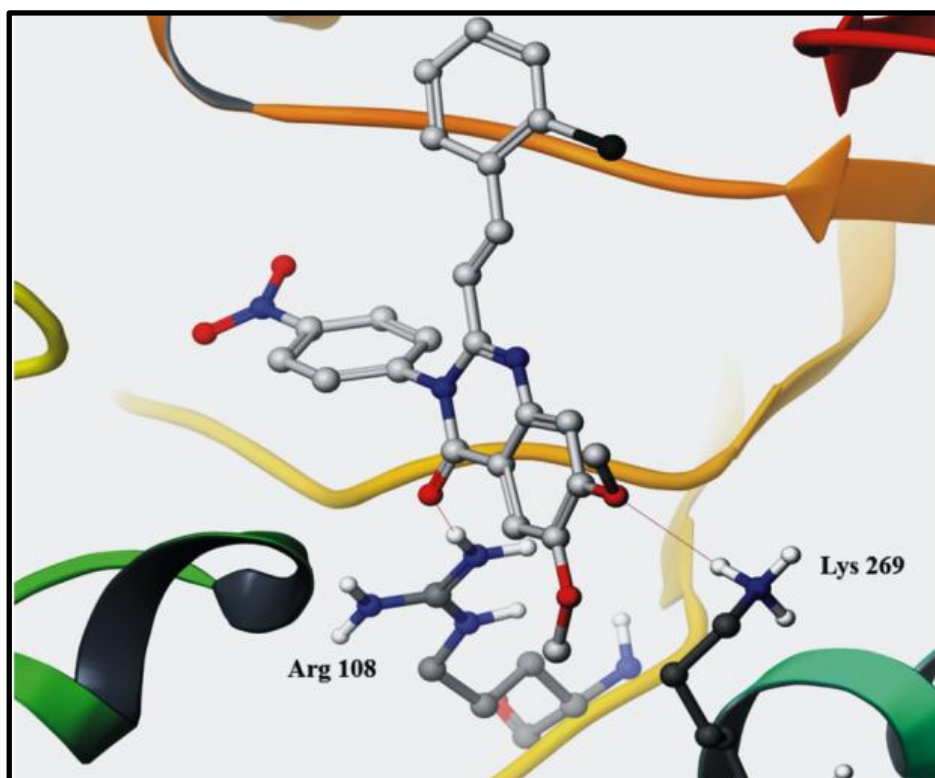


**Figure 5C.2.1.** Compound **5g** hydrogen bonded with key amino acid residues (Arg 108 and Lys 269) shown as ball and stick model. Hydrogen bonds are displayed as dashed magenta.

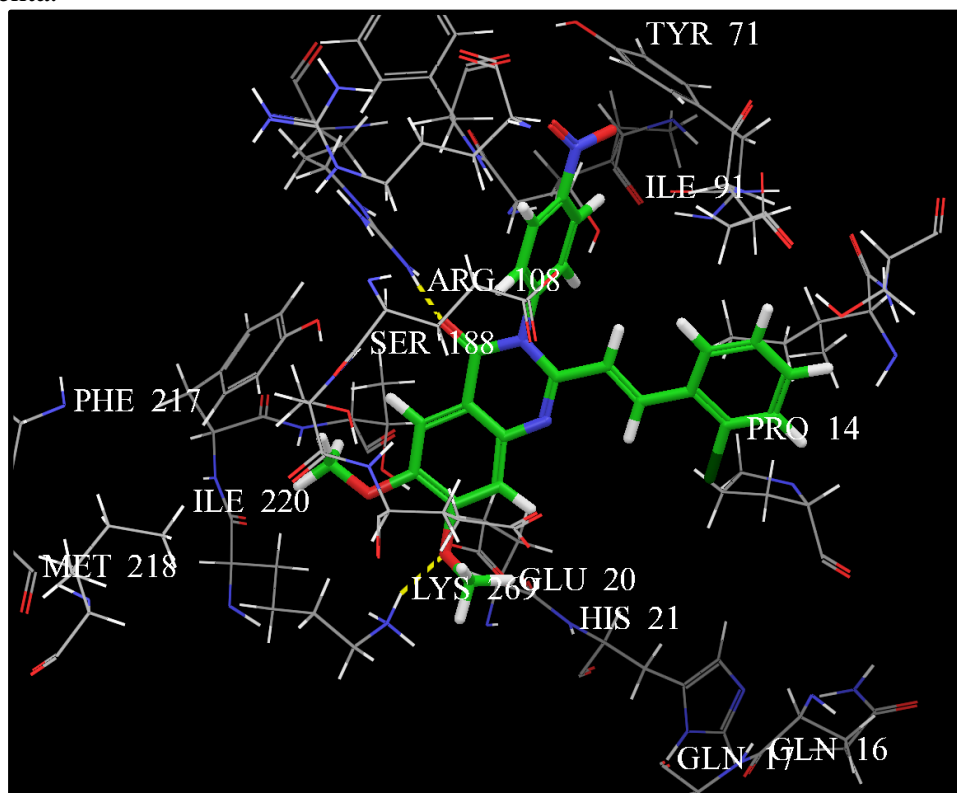


**Figure 5C.2.2.** Compound **5g** docked within the predicted binding pocket of ATD of glutamate receptor. The key amino acid shown within the cavity forming loop are Gln 16, Gln 17, Glu 20, His 21, Tyr 71, Ile 91, Arg 108, Ser 188, Phe 217, Met 218, Ile 220 and Lys 269. Hydrogen bonds are shown as yellow dash.

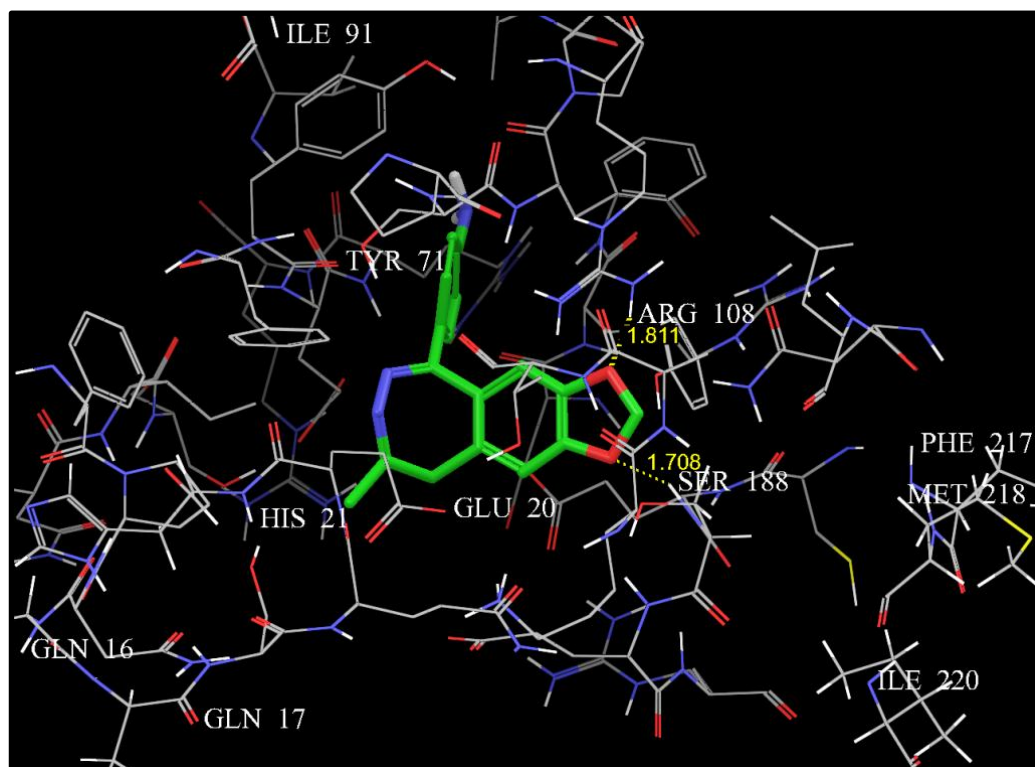


**Figure 5C.2.3.** GYKI 52466 docked within the predicted binding pocket of ATD of glutamate receptor. Hydrogen bonds are shown as yellow dash and bonded with ARG 108 and SER 188.

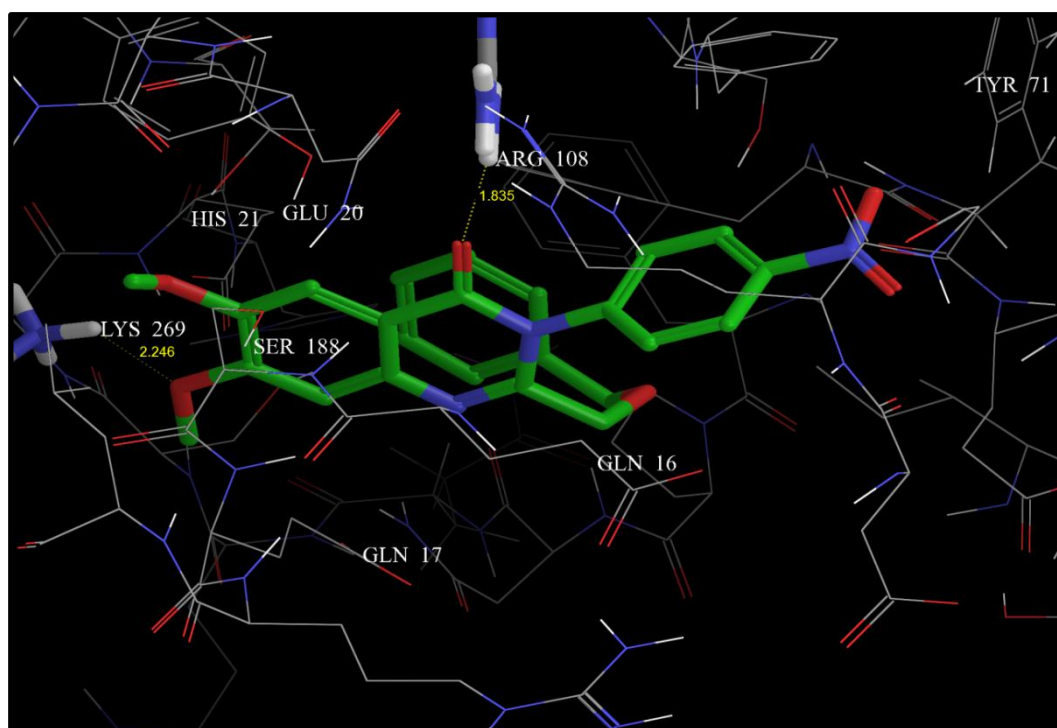


**Figure 5C.2.4.** Compound **8f** docked within the predicted binding pocket of ATD of glutamate receptor. The key amino acid shown within the cavity forming loop are Gln 16, Gln 17, Glu 20, His 21, Tyr 71, Arg 108, Ser 188 and Lys 269. Hydrogen bonds are shown as yellow dash.

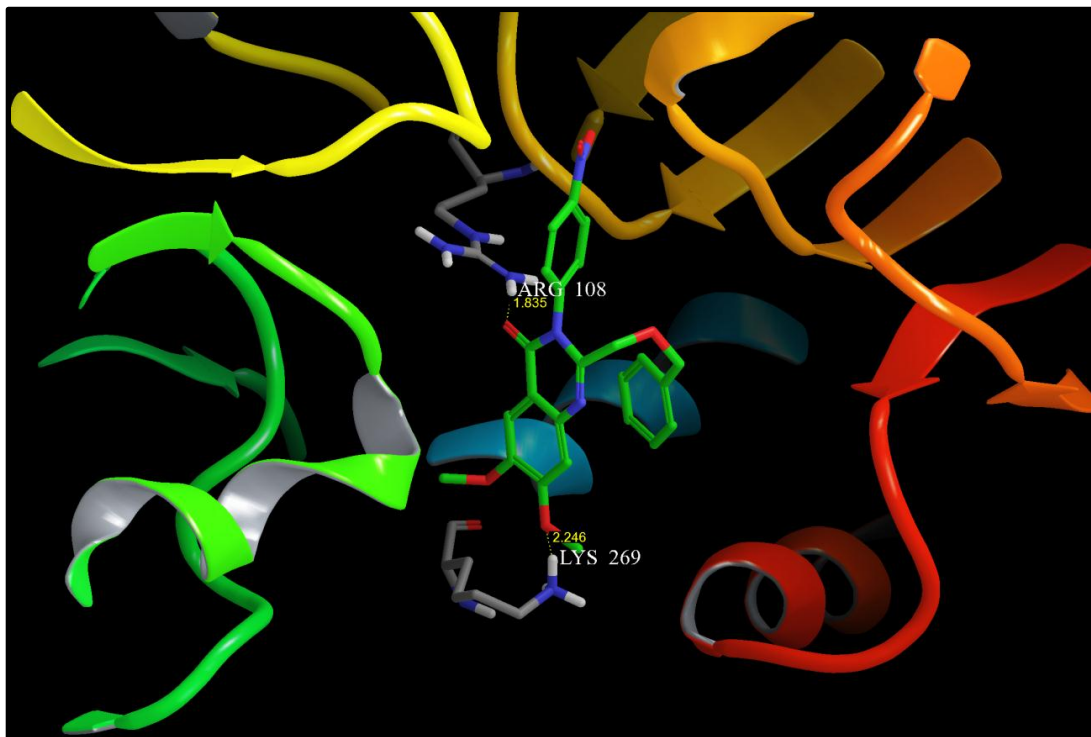


**Figure 5C.2.5.** Compound **8f** within the binding cavity formed by loop residues and hydrogen bonded with ARG 108 and LYS 269.